

Solid state multicolor emission in substitutional solid solutions of metal-organic frameworks

Wesley J. Newsome, Suliman Ayad, Jesus Cordova, Eric W. Reinheimer, Andres D Campiglia, James K. Harper, Kenneth Hanson, and Fernando J. Uribe-Romo

J. Am. Chem. Soc., **Just Accepted Manuscript** • DOI: 10.1021/jacs.9b05191 • Publication Date (Web): 20 Jun 2019

Downloaded from <http://pubs.acs.org> on June 20, 2019

Just Accepted

“Just Accepted” manuscripts have been peer-reviewed and accepted for publication. They are posted online prior to technical editing, formatting for publication and author proofing. The American Chemical Society provides “Just Accepted” as a service to the research community to expedite the dissemination of scientific material as soon as possible after acceptance. “Just Accepted” manuscripts appear in full in PDF format accompanied by an HTML abstract. “Just Accepted” manuscripts have been fully peer reviewed, but should not be considered the official version of record. They are citable by the Digital Object Identifier (DOI®). “Just Accepted” is an optional service offered to authors. Therefore, the “Just Accepted” Web site may not include all articles that will be published in the journal. After a manuscript is technically edited and formatted, it will be removed from the “Just Accepted” Web site and published as an ASAP article. Note that technical editing may introduce minor changes to the manuscript text and/or graphics which could affect content, and all legal disclaimers and ethical guidelines that apply to the journal pertain. ACS cannot be held responsible for errors or consequences arising from the use of information contained in these “Just Accepted” manuscripts.

Solid state multicolor emission in substitutional solid solutions of metal-organic frameworks

Wesley J. Newsome,^{1§} Suliman Ayad,^{2§} Jesus Cordova,¹ Eric W. Reinheimer,³ Andres D. Campiglia,¹ James K. Harper,¹ Kenneth Hanson,^{2*} Fernando J. Uribe-Romo.^{1*}

¹Department of Chemistry, University of Central Florida, 4111 Libra Dr. Rm. 251 PSB, Orlando, FL 32816-2366, USA.

²Department of Chemistry & Biochemistry, Florida State University, 95 Chieftan Way, Tallahassee, FL 32306-4390, USA.

³Rigaku Americas Corporation, 9009 New Trails Dr., The Woodlands, TX 77381, USA.

§ = Equal contribution.

White light emission, Structure-property relationship, Broadband fluorescence

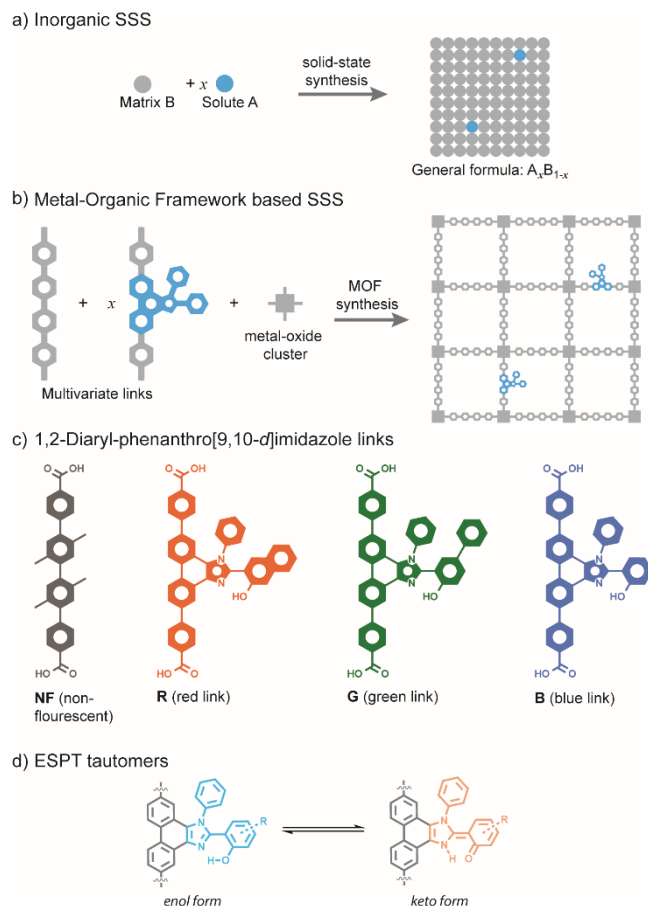
ABSTRACT: Preparing crystalline materials that produce tunable organic-based multicolor emission is a challenge, due to the inherent inability to control the packing of organic molecules in the solid state. Utilizing multivariate, high symmetry metal-organic frameworks, MOFs, as matrices for organic-based substitutional solid solutions allows for the incorporation of multiple fluorophores with different emission profiles into a single material. By combining non-fluorescent links with dilute mixtures of red, green, and blue fluorescent links we prepared zirconia-type MOFs and found that the bulk materials exhibit features of solution-like fluorescence. Our study found that MOFs with fluorophore link concentration of around 1 mol% exhibit fluorescence with decreased inner filtering, demonstrated by changes in spectral profiles, increased quantum yields, and lifetime dynamics expected for excited state proton transfer emitters. Our findings enabled us to prepare organic-based substitutional solid solutions with tunable chromaticity regulated only by the initial amounts of fluorophores. These materials emit multicolor and white light with high quantum yields (~2-14%), high color rendering indices (>93), long shelf life, and superb hydrolytic stability at ambient conditions.

Introduction

Multicolor emission in solutions is a phenomenon that occurs in a system of multiple emitters, where the bulk fluorescence of a solution is the result of the combined emission of each emitter.¹⁻² In liquid solutions of dilute organic fluorophores, this phenomenon is easily controlled, because solutions with exact concentrations can be prepared. In the crystalline solid-state (*i.e.*, excluding polymer blends and glasses), organic-based multicolor emission is more challenging to produce, because when the solvent is removed, mixtures of organic fluorophores aggregate,³⁻⁴ phase separate, and quench, producing heterogeneous solid mixtures with unpredictable fluorescence. A strategy to produce organic-based crystals with tunable bulk multicolor emission is by adapting the solid-state chemistry concept of substitutional solid solutions (SSS). SSS are crystals that form when a solute atom (Figure 1a) is incorporated into a uniform crystalline matrix, substituting some of the matrix atoms, so the solute is effectively dissolved within the average unit cell.⁵ Application of this concept in inorganic materials has allowed for fine-tuned control of physical properties of materials for applications such as lasers⁶ and blue LEDs.⁷ In the case of organic materials, however, the concept of preparing SSS does not generally apply for several reasons. First, unlike atoms, organic molecules are non-spherical, so matrix-dopant

matching is a non-trivial task.⁸⁻⁹ Second, organic compounds tend to form low symmetry and unpredictable crystal packings,¹⁰ which makes their bulk crystallographic characterization a challenge. Third, as mentioned above, mixtures of organic compounds phase separate during crystallization, so homogeneous incorporation of solutes is not ensured. Despite these challenges, preparation of organic-based SSS with tunable fluorescence would allow for preparing crystalline materials that take advantage of the inherent tunability of molecular emitters.

Multivariate metal-organic frameworks (MTV MOFs) are a sub-class of MOFs where organic links of varied functionalization are incorporated into a single phase MOF.¹¹ These types of MOFs are an attractive platform for making multicolor emitting crystals because the crystalline arrangement of the organic links is dictated by the structure of the MOF. When considering high-symmetry MOFs, the organic links will also arrange in a high symmetry environment despite their differences in chemical functionality (Figure 1b).¹² Here, we demonstrate that utilizing high-symmetry multivariate MOFs as matrices for organic-based SSS enables the preparation of crystalline multicolor emitting materials. By forcing the organic links to arrange in high symmetry environments,



30
31
32
33

Figure 1 (a) Scheme of inorganic-based substitutional solid solution (b) Scheme of organic-based substitutional solid solution formation in MOFs. (c) Organic links used in this study. (d) Excited state proton transfer (ESPT) *enol* and *keto* tautomers.

34
35
36
37
38
39
40
41
42
43
44
45
46
47
48
49
50
51
52
53
54
55
56
57

a higher level of synthetic control can be achieved, because these MTV MOFs circumvent the problems associated with organic-based SSS (see above). Also using high symmetry MOFs (*e.g.* cubic) facilitates crystallographic characterization via crystal simulations and powder diffractometry. We demonstrate that incorporation of links that contain red, green and blue (RGB) fluorescent moieties (Figure 1b) into a non-fluorescent, high-symmetry MOF, results in the formation of fluorescent, organic-based SSS. The observed organic SSS behavior allows tunable multicolor emission in bulk crystals with emissive properties dictated exclusively by the input concentration of RGB fluorophore links, producing materials that fluoresce with many different colors, including white light, with easy-to-tune color parameters (*e.g.* chromaticity and white-light temperature), and very high color rendering indices. The prepared materials retain their crystallinity at room temperature for months under normal laboratory conditions, and even after direct exposure to water. We found that dilution of fluorescent links at around 1.0 mol% displayed typical solution behavior, including decreased inner filtering, high quantum yields, tunable chromaticities, excitation-emission independence, concentration dependent energy transfer, as well as emission phenomena expected from the fluorophores, such as excited-state proton transfer (ESPT).

The MOF matrix utilized here consists on the zirconia-type PPPP-PIZOF MOF (Figure S1), an interwoven face-centered cubic network (space group $Fd\bar{3}m$)¹³ built with tetramethyl quarterphenyldicarboxylate (Figure 1c) that is non-fluorescent in the visible region. This MOF type is water stable and allows for the incorporation of links of varied nature.¹² Based on ESPT dyes designed by Park *et al.*, the multivariate links are composed of quarterphenyl chains bearing 1,2-diarylphenanthro[9,10-*d*]imidazole fluorophores.¹⁴⁻¹⁵ This moiety was utilized as a template for its stability to MOF synthetic conditions, high quantum yield, and ease of color variability through synthesis. When the aryl at the 2 position is an *o*-phenol derivative, the dye can exist as an *enol* or *keto* tautomer (Figure 1d) by transferring the phenolic proton to the unsubstituted nitrogen of the imidazole ring.¹⁶ In the ground state, these dyes exist in the *enol* tautomer. After excitation, a proton transfer can occur producing the excited state *keto* form that induces a large apparent Stokes shift, that varies according to the molecular structure of the phenol. As such, an unsubstituted phenol has a small shift, emitting in the blue, adding a phenyl group shifts emission to green, and changing to a naphthol group further shifts emission to red. After relaxing via emission, the dye readily reverts to the *enol* form. This large apparent Stokes shift is advantageous for mixed fluorophore systems because it allows for single wavelength excitation of the high energy

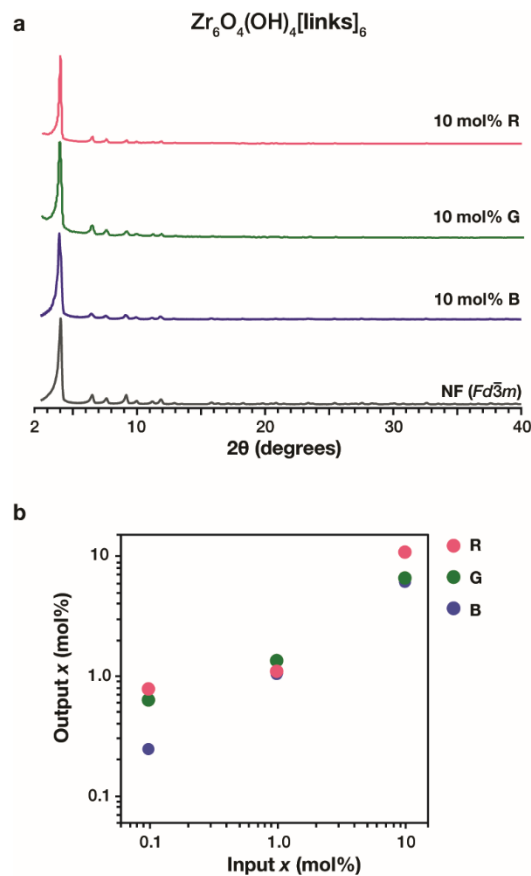


Figure 2 (a) Powder X-ray diffraction (PXRD) patterns of **NF** and **RGB**-containing MOFs, indicating their isorecticular nature. (b) Substitutional input-output plot for 3 sets of single fluorophore MOFs with x in mol%.

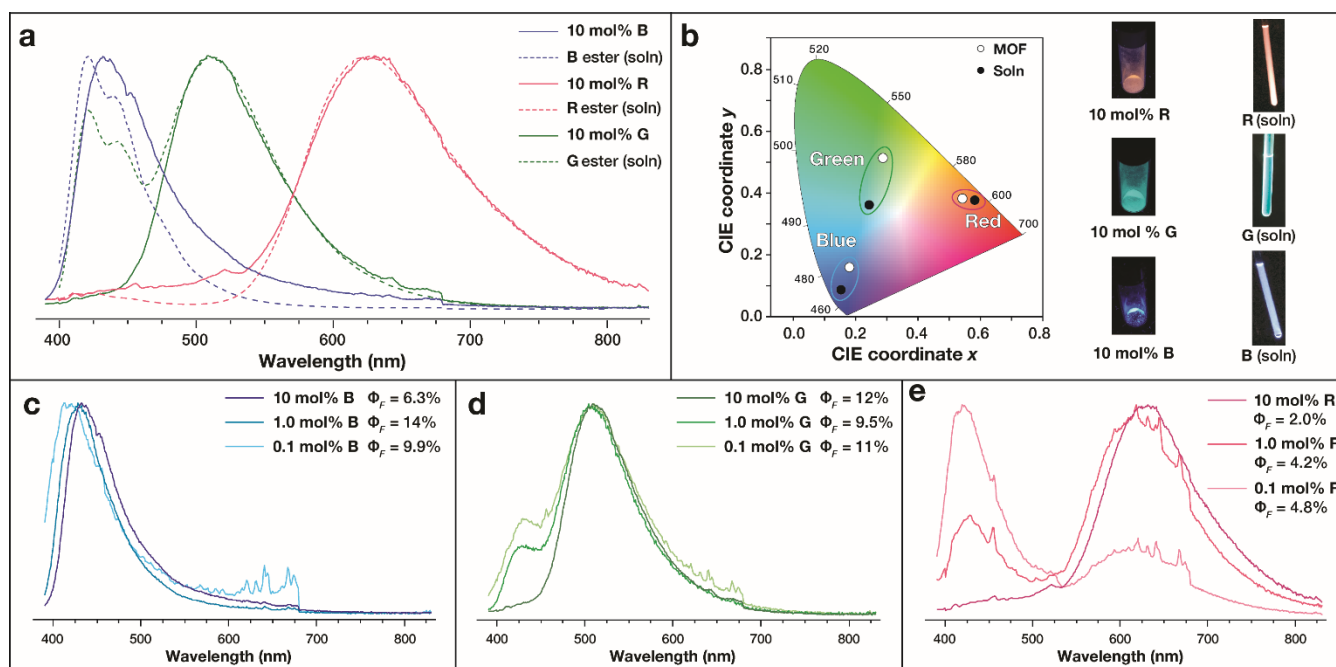


Figure 3 (a) Overlay of toluene-solvated fluorophore esters (compounds S7, S13, and S16, dashed lines) and $x = 10$ mol% input single fluorophore MOFs (solid lines). (b) CIE chromaticity coordinates of prepared $x = 10$ mol% MOFs (open circles) and solvated ester links (closed circles), and optical image of MOF powders and solvated links under UV light. (c-e) Emission profiles of **B**, **G**, and **R** MOFs, respectively at varied dilution ($0.1 \leq x \leq 10$ mol%) indicating their excited-state lifetimes and quantum yields ($\lambda_{exc} = 365$ nm).

enol form and emission from the low energy *keto* form with minimal spectral overlap.¹⁶⁻¹⁷ Furthermore, covalent attachment of diaryl-phenanthroimidazole to the quater-phenyl links ensures that fluorophores will not diffuse or leach out of the solid.¹⁸⁻¹⁹ The SSS were prepared using the multivariate links shown in Figure 1b, herein referred to as **NF** (non-fluorescent), **R** (red), **G** (green), and **B** (blue).

Results and Discussion

Crystalline single fluorophore MOFs of **NF** with **R**, **G**, or **B** produced solids samples with formulas $Zr_6O_4(OH)_4[R_xNF_{1-x}]_6$, $Zr_6O_4(OH)_4[G_xNF_{1-x}]_6$, and $Zr_6O_4(OH)_4[B_xNF_{1-x}]_6$ with substituent input x values between 0.10 and 10 mol% (See SI for methods). For simplicity, samples with a single fluorophore will be referred to as $x\%$ -fluorophore, *i.e.*, **10%-B**, **10%-G**, and **10%-R** for MOFs with a 10% fluorophore input. All samples were prepared utilizing solvothermal MOF crystallization conditions¹³ and exhibited the same powder X-ray diffraction (PXRD) pattern of the pure **NF** MOF (Figure 2a). Predictable and adjustable linker incorporation was demonstrated from the synthetic input/structural output plot shown in Figure 2b with output composition values determined by solution ¹H NMR of digested MOF samples (Section S6). Attempts to prepare MOFs with higher fluorophore content (>10 mol%) were unsuccessful, producing amorphous, non-porous solids with inconsistent fluorophore content. This observation indicates that the MOF matrix has a limited tolerance for sterically crowded links. Furthermore, it also suggests that it is unlikely that a mix-phase MOF composite is formed (*e.g.*, clustered **RGB** MOF crystals mixed with pure **NF** MOF crystals). Regarding the homogeneity of the fluorescent

links in the SSS, previous work on high-symmetry MTV MOFs has shown that the distribution of the MTV links is highly dependent on the dilution range of the dopant link. In our case, high fluorophore dilution likely results in MOF with homogeneous distribution,¹² with the 10 mol% MOFs potentially forming alternating apportionments.²⁰ Further studies using multidimensional solid-state NMR on isotopically enriched MOFs will provide this information. Nonetheless, consistent and reproducible fluorescence was observed in the bulk, indicating little effect from the links distribution.

Despite having similar absorption profiles (Figure S2), upon excitation at 365 nm, MOFs made with **10%-R**, **10%-G**, and **10%-B**, exhibit solid-state emission maxima at 430, 510, and 630 nm (Figure 3a), respectively, with relatively high color purity (Figure 3b). The emission profiles of these MOFs are drastically different than the neat solid linkers (Figure S3). In contrast, the low energy *keto* emission in the MOFs closely resembles that of the ester forms of the RGB links solvated in toluene (Figure 3a, dashed lines), suggesting that the pore microenvironment of the MOF more closely resembles the toluene-solvated, rather than neat solids of the linker.

The fluorophore mimics liquid-phase solution behavior in that the RGB links show concentration dependent changes in the emission profiles for all three fluorophore MOFs (Figure 3c-e). These changes are most notable in **R** and **G** containing MOFs, where there is a gradual increase in the high energy *enol* emission with decreasing concentration and a shift in the CIE (Commission Internationale de l'Éclairage) chromaticity coordinates from the red and green

regions towards the blue portion of the diagram (Figure S4). For **B** and **R**, the spectral changes are accompanied by an emission lifetime and quantum yield increase from $x = 10$ to 1.0 mol% (Figure 3c and 3e, Table S3). These observations are consistent with an energy transfer event²¹ where spectral overlap between *enol* emission and *enol* absorption inhibits the higher energy light from exiting the solid. A similar effect can be observed in concentrated solutions but is presumably greatly enhanced by the high local concentration of the fluorophores in the MOF.²² Monitoring the excited state dynamics in the MOF using sub-nanosecond transient absorption measurements will be necessary to definitively establish an energy transfer mechanism. Regardless, the similarity in lifetime and quantum yield between **1.0%-B** and **0.1%-B**, as well as, **1.0%-R** and **0.1%-R** (Figure 3c and 3e) suggests that the inner filtering effect is minimal at concentrations of $x = 1.0$ mol%. These concentrations of fluorophore result in MOFs with quantum yields which are up to an order of magnitude greater than previously prepared broadband emitting MOFs,²³⁻²⁵ and are similar to the soluble ester forms of the linkers in a toluene solution (Table S2).

This dilution can be interpreted in terms of molar concentration of the links in the MOF, since $[\text{links}]_{\text{max}} = 1.34 \text{ M}$ (single crystal analysis of **NF** MOF evidences 48 links per unit cell with a cell volume of $58,400 \text{ \AA}^3$, equivalent to $1.34 \text{ mol}_{\text{links}} \text{ dm}^{-3}$). As such, **10%-B**, **1.0%-B**, and **0.1%-B** have molar concentrations of $[\text{B}] = 134 \text{ mM}$, 13.4 mM , and 1.34 mM , respectively. These molarity values for **1.0%-B** and **0.1%-B** fall close to a dilution range with reduced inner filtering, and the **10%-B** resembles a concentrated solution where the emission is dominated by this inner filtering.

Incorporation of two and three fluorophores resulted in MOFs that exhibit the combined emission of each fluorophore. For $\text{Zr}_6\text{O}_4(\text{OH})_4(\text{R}_x\text{B}_{1-x})_y\text{NF}_{1-y}$, $\text{Zr}_6\text{O}_4(\text{OH})_4(\text{G}_x\text{B}_{1-x})_y\text{NF}_{1-y}$ with $y = 0.01$, under 365 nm excitation, we observed a sum of the individual components and a linear transition from **R** to **B** or **G** to **B** as x varies from 0.9 to 0.1 (Figure 4). The excitation-emission maps (Figure S5) as well as CIE coordinate diagrams with respect to λ_{ex} (Figure S4) indicate that emission from the mixed fluorophore systems are excitation wavelength independent. The additive nature of the emission profiles and the wavelength independent CIE chromaticity coordinates are consistent with minimal energy transfer in the $y = 0.01$ MOFs. Consequently, selective color generation along these axes could be achieved by tuning the fluorophore ratio.

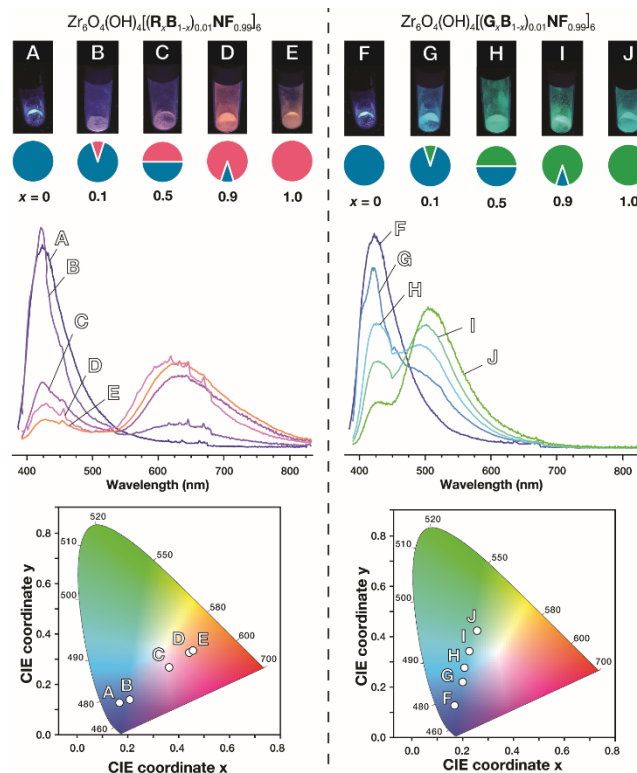


Figure 4 Two component SSS MOFs: (Top) Optical images of samples under $\lambda_{\text{ex}} = 365 \text{ nm}$ indicating their fluorophore composition, (middle) emission profiles with $\lambda_{\text{ex}} = 365 \text{ nm}$, and (bottom) CIE chromaticity coordinates of mixtures of **R** and **B** (left), and mixtures of **G** and **B** (right).

The three-fluorophore system with a composition of $\text{Zr}_6\text{O}_4(\text{OH})_4(\text{R}_x\text{G}_{1-2x}\text{B}_x)_y\text{NF}_{1-y}$, exhibited emission profiles that depend on the total fluorophore concentration y . As expected for $y = 0.10$, the emission is strongly dependent on the excitation wavelength (Figure S6-8) and generally dominated by yellow emission (**R** + **G**) with minimal high energy contribution (**B**) due to strong inner filter effects. For the $\text{Zr}_6\text{O}_4(\text{OH})_4[(\text{R}_{0.33}\text{G}_{0.33}\text{B}_{0.33})_{0.10}\text{NF}_{0.90}]_6$ MOF (Figure S7 and Table S3), excited state lifetimes for **B** ($\tau_{460 \text{ nm}} = 1.5 \text{ ns}$), **G** ($\tau_{560 \text{ nm}} = 1.8 \text{ ns}$), and **R** ($\tau_{660 \text{ nm}} = 1.9 \text{ ns}$) were similar to that of **10%-R** ($\tau_{660 \text{ nm}} = 1.5 \text{ ns}$) but notably shorter than for **10%-G** ($\tau_{560 \text{ nm}} = 3.1 \text{ ns}$) and **10%-B** ($\tau_{460 \text{ nm}} = 5.7 \text{ ns}$). The similarity in lifetimes of the three peaks is symptomatic of an energy transfer equilibrium condition where the collective emission decay kinetics are dictated by the emitter with the fastest radiative decay rate (*i.e.*, **R**).²⁶ That is, **B** energy transfer to **R** and **G**, **G** *enol* energy transfer to **R** and **B**, and **R** *enol* energy transfer to **G** and **B**, with all these processes occurring in parallel. In contrast, an overall fluorophore link dilution to 1.0 mol%, $\text{Zr}_6\text{O}_4(\text{OH})_4(\text{R}_{0.33}\text{G}_{0.33}\text{B}_{0.33})_{0.01}\text{NF}_{0.99}$, resulted in lifetimes of 3.9, 2.6, and 1.6 ns for **B**, **G**, and **R**, respectively, more closely resemble the single component systems with no energy transfer.

The excitation-emission maps (Figure S5) show a decrease in excitation wavelength dependence, as seen in other dilute samples. At these lower concentrations an increase in the *enol* emission is observed, most strongly for **R**, which results in deviations from the linear trend in the CIE chro-

maticity coordinates (points L and M, Figure 5). Once the concentration of **R** is sufficiently increased ($\text{Zr}_6\text{O}_4(\text{OH})_4(\text{R}_{0.4}\text{G}_{0.2}\text{B}_{0.4})_{0.01}\text{NF}_{0.99}$) the low energy *keto* emission becomes predominant (Figure 5, point N). This sample exhibits the combined broadband emission from **RGB**, with CIE chromaticity coordinates close to the center of the white light region (0.31, 0.33), a quantum yield of 4.3%, and a correlating black-body temperature of 6480 K. This temperature is nearly identical to that of natural daylight (6500 K)²⁷ and can be adjusted based on the fluorophore concentration or the ratio of the fluorescent links. By increasing the overall concentration of the fluorophores to 10% a warmer white light can be achieved in $\text{Zr}_6\text{O}_4(\text{OH})_4[(\text{R}_{0.40}\text{G}_{0.20}\text{B}_{0.40})_{0.10}\text{NF}_{0.90}]_6$ which has CIE chromaticity coordinates of (0.43, 0.39) and a corresponding temperature of 3060 K. Additionally, utilizing a two component system, taking advantage of the low concentration *enol* emission from **R**, cool white light can be achieved in $\text{Zr}_6\text{O}_4(\text{OH})_4[(\text{R}_{0.5}\text{G}_{0.5})_{0.01}\text{NF}_{0.99}]_6$ with CIE chromaticity coordinates of (0.29, 0.33) and a corresponding temperature of 7820 K (Figure S9). To our knowledge, this is the first example of crystalline bulk materials whose fluorescent properties were adjusted following the dilution strategies used in liquid phase fluorescence.

As a compliment to the CIE coordinates, the color rendering index (CRI) is a critical parameter in describing how faithfully a light source represents the true color of an object with a score of 100 being a source identical to standardized daylight.²⁸ The CRI values for the above white light MOFs were calculated and the results are reported in Table S4. Remarkably, sample N with formula $\text{Zr}_6\text{O}_4(\text{OH})_4(\text{R}_{0.4}\text{G}_{0.2}\text{B}_{0.4})_{0.01}\text{NF}_{0.99}$ demonstrated a CRI of 93 and the two component **R/G** system with formula $\text{Zr}_6\text{O}_4(\text{OH})_4(\text{R}_{0.5}\text{G}_{0.5})_{0.01}\text{NF}_{0.99}$ had a CRI of 95. For context, typical fluorescent bulbs are around 50 and white LEDs often score >80.²⁹ These results indicate that the mixed emitter MOFs are capable of both tunable emission chromaticity, as well as accurate color rendition.

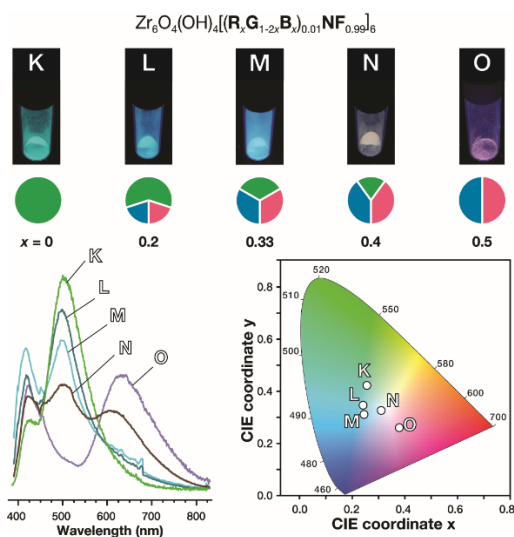


Figure 5 Three component SSS MOFs: (Top) Optical images of samples under $\lambda_{\text{ex}} = 365$ nm indicating their fluorophore composition, (bottom left) emission profiles with λ_{ex}

= 365 nm, and (bottom right) CIE chromaticity coordinates of each sample.

All the MOFs synthesized are porous, stable to water, humidity, and up to 400 °C (Figure S91), and also completely composed of earth-abundant elements. For example, **10%-B** and $\text{Zr}_6\text{O}_4(\text{OH})_4[(\text{R}_{0.33}\text{G}_{0.33}\text{B}_{0.33})_{0.01}\text{NF}_{0.99}]_6$ have Brunauer–Emmett–Teller (BET) surface areas of $S_{\text{BET}} = 1620$ and $1600 \text{ m}^2 \text{ g}^{-1}$ respectively (Table S6). Water stability in **10%-B** was demonstrated by following changes in the diffraction pattern (Figure S56) and BET surface area before and after exposure to water (Figure S56-57 and Table S6). Furthermore, the long-shelf life of the materials was demonstrated by the lack of changes in their PXRD even after 10 months of storage under laboratory conditions (Figure S58 for **10%-B**).

Other methods utilizing metal-organic materials for preparation of solid-state emission often bring significant drawbacks. For instance, Cu_4I_4 is a cluster used to create emissive materials, which has become a growing field in recent years. These materials offer similar quantum yields for pure colors, *ca.* 9%,³⁰⁻³¹ but crystallize in low symmetry, unpredictable space groups. The Cu_4I_4 cluster is less rigid compared to the zirconium cluster, which results in cluster deformation when different ligands are bound creating low symmetry complex crystal systems.³²⁻³³ Other emissive materials include MOFs where all the organic links in the framework are emissive fluorophores.³⁴ This results in unpredictable and inefficient fluorescence due to high inner filtering effects present in the material. Impregnating MOFs with fluorescent guest dyes can produce multicolor emission;¹⁹ however, guest diffusion raises questions of homogeneity and long-term stability of the materials. Other MOF-based emissive materials utilize expensive rare-earth elements to achieve green and red fluorescence, with quantum yields ranging from 2-50%;³⁵⁻³⁷ yet, rare-earth elements are unsustainable, limiting their use as applied materials in the long term.³⁸ As such, the MOFs and methodology presented herein offer: an ease of characterization due to the high symmetry crystal system, tunable fluorophore concentration to achieve higher quantum yields with less inner filtering, and using earth abundant elements.

Conclusions

Applying the concept of SSS to organic-based materials was accomplished using high symmetry MOFs as matrices. This approach allows for circumvention of common challenges associated with emissive MOFs including: high inner filtering effects that cause complex emission, due to high fluorophore concentration, and high synthetic costs due to inclusion of lanthanides. This approach will further enable the ability to study other similar organic-based molecular phenomena in solids, and can provide organic-based SSS materials for high precision applications such as in photonic devices, and high-definition displays.

ASSOCIATED CONTENT

Supporting Information. Materials and methods, full materials and photophysical characterization, single crystal crystal-

lographic information file. This material is available free of charge via the Internet at <http://pubs.acs.org>.

AUTHOR INFORMATION

Corresponding Author

fernando@ucf.edu, and hanson@chem.fsu.edu

Author Contributions

The manuscript was written through contributions of all authors. All authors have given approval to the final version of the manuscript.

Funding Sources

Synthesis of materials (CHE-1665257, FJU-R) and Photophysical measurements (CHE-1531629, KH) were supported by the National Science Foundation.

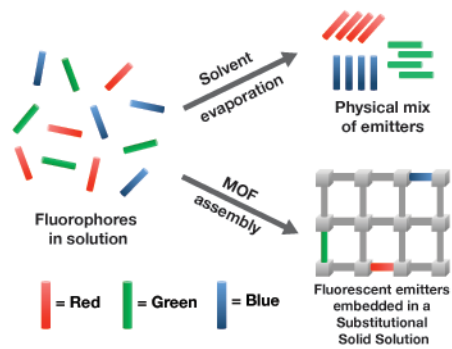
ACKNOWLEDGMENTS

We would like to thank Dr. Mark Maric (UCF) for technical assistance and Dr. Titel Jurca (UCF) for helpful discussions.

REFERENCES

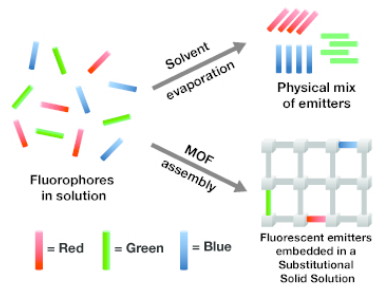
- Görl, D.; Zhang, X.; Würthner, F., Molecular Assemblies of Perylene Bisimide Dyes in Water. *Angewandte Chemie International Edition* **2012**, *51* (26), 6328-6348.
- Huo, S.; Duan, P.; Jiao, T.; Peng, Q.; Liu, M., Self-Assembled Luminescent Quantum Dots To Generate Full-Color and White Circularly Polarized Light. *Angewandte Chemie International Edition* **2017**, *56* (40), 12174-12178.
- Ryu, J.-H.; Hong, D.-J.; Lee, M., Aqueous self-assembly of aromatic rod building blocks. *Chemical Communications* **2008**, (9), 1043-1054.
- Kaesler, A.; Schenning, A. P. H. J., Fluorescent Nanoparticles Based on Self-Assembled π -Conjugated Systems. *Advanced Materials* **2010**, *22* (28), 2985-2997.
- West, A. R., "Solid solutions" in *solid state chemistry and its applications* Wiley and Sons: 1984.
- Maiman, T. H., Stimulated optical radiation in ruby. *Nature* **1960**, *187* (4736), 493-494.
- Nakamura, S.; Mukai, T.; Senoh, M., Candela-class high-brightness InGaN/AlGaIn double-heterostructure blue-light-emitting diodes. *Applied Physics Letters* **1994**, *64* (13), 1687-1689.
- Desiraju, G. R., Crystal engineering: from molecule to crystal. *Journal of the American Chemical Society* **2013**, *135* (27), 9952-9967.
- Zhen, Y.; Tanaka, H.; Harano, K.; Okada, S.; Matsuo, Y.; Nakamura, E., Organic Solid Solution Composed of Two Structurally Similar Porphyrins for Organic Solar Cells. *Journal of the American Chemical Society* **2015**, *137* (6), 2247-2252.
- Price, S. L., Control and prediction of the organic solid state: a challenge to theory and experiment. *Proceedings of the Royal Society A: Mathematical, Physical and Engineering Sciences* **2018**, *474* (2217), 20180351.
- Deng, H.; Doonan, C. J.; Furukawa, H.; Ferreira, R. B.; Towne, J.; Knobler, C. B.; Wang, B.; Yaghi, O. M., Multiple functional groups of varying ratios in metal-organic frameworks. *Science* **2010**, *327* (5967), 846-850.
- Schrimpf, W.; Jiang, J.; Ji, Z.; Hirschle, P.; Lamb, D. C.; Yaghi, O. M.; Wuttke, S., Chemical diversity in a metal-organic framework revealed by fluorescence lifetime imaging. *Nature Communications* **2018**, *9* (1), 1647.
- Lippke, J.; Brosent, B.; von Zons, T.; Virmani, E.; Lilienthal, S.; Preuße, T.; Hülsmann, M.; Schneider, A. M.; Wuttke, S.; Behrens, P.; Godt, A., Expanding the group of porous interpenetrated Zr-organic frameworks (PZOFs) with linkers of different lengths. *Inorganic Chemistry* **2017**, *56* (2), 748-761.
- Nayak, M. K., Synthesis, characterization and optical properties of aryl and diaryl substituted phenanthroimidazoles. *Journal of Photochemistry and Photobiology A: Chemistry* **2012**, *241*, 26-37.
- Park, S.; Kwon, J. E.; Park, S. Y., Strategic emission color tuning of highly fluorescent imidazole-based excited-state intramolecular proton transfer molecules. *Physical Chemistry Chemical Physics* **2012**, *14* (25), 8878-8884.
- Kwon, J. E.; Park, S.; Park, S. Y., Realizing molecular pixel system for full-color fluorescence reproduction: RGB-emitting molecular mixture free from energy transfer crosstalk. *Journal of the American Chemical Society* **2013**, *135* (30), 11239-11246.
- Kwon, J. E.; Park, S. Y., Advanced organic optoelectronic materials: harnessing excited-state intramolecular proton transfer (ESIPT) process. *Advanced Materials* **2011**, *23* (32), 3615-3642.
- Han, S.; Wei, Y.; Valente, C.; Lagzi, I.; Gassensmith, J. J.; Coskun, A.; Stoddart, J. F.; Grzybowski, B. A., Chromatography in a single metal-organic framework (MOF) crystal. *Journal of the American Chemical Society* **2010**, *132* (46), 16358-16361.
- Ullman, A. M.; Brown, J. W.; Foster, M. E.; Léonard, F.; Leong, K.; Stavila, V.; Allendorf, M. D., Transforming MOFs for Energy Applications Using the Guest@MOF Concept. *Inorganic Chemistry* **2016**, *55* (15), 7233-7249.
- Kong, X.; Deng, H.; Yan, F.; Kim, J.; Swisher, J. A.; Smit, B.; Yaghi, O. M.; Reimer, J. A., Mapping of Functional Groups in Metal-Organic Frameworks. *Science* **2013**, *341* (6148), 882-885.
- Valeur, B., *Molecular fluorescence*. 1 ed.; Wiley-VCH: Weinheim, Germany, 2002.
- Zhao, J.; Ji, S.; Chen, Y.; Guo, H.; Yang, P., Excited state intramolecular proton transfer (ESIPT): from principal photophysics to the development of new chromophores and applications in fluorescent molecular probes and luminescent materials. *Physical Chemistry Chemical Physics* **2012**, *14* (25), 8803-8817.
- He, J.; Zeller, M.; Hunter, A. D.; Xu, Z., White Light Emission and Second Harmonic Generation from Secondary Group Participation (SGP) in a Coordination Network. *Journal of the American Chemical Society* **2012**, *134* (3), 1553-1559.
- Haider, G.; Usman, M.; Chen, T.-P.; Perumal, P.; Lu, K.-L.; Chen, Y.-F., Electrically Driven White Light Emission from Intrinsic Metal-Organic Framework. *ACS Nano* **2016**, *10* (9), 8366-8375.
- Qu, M.; Li, H.; Zhao, Y.; Zhang, X.-M., Single-Component Color-Tunable Gd(pic)₃: Eu³⁺ Phosphor Based on a Metal-Organic Framework for Near-UV White-Light-Emitting Diodes. *ACS Omega* **2019**, *4* (2), 3593-3600.
- Zhou, C.; Yuan, L.; Yuan, Z.; Doyle, N. K.; Dilbeck, T.; Bahadur, D.; Ramakrishnan, S.; Dearden, A.; Huang, C.; Ma, B., Phosphorescent Molecular Butterflies with Controlled Potential-Energy Surfaces and Their Application as Luminescent Viscosity Sensor. *Inorganic Chemistry* **2016**, *55* (17), 8564-8569.
- Judd, D. B.; MacAdam, D. L.; Wyszecki, G.; Budde, H. W.; Condit, H. R.; Henderson, S. T.; Simonds, J. L., Spectral Distribution of Typical Daylight as a Function of Correlated Color Temperature. *J. Opt. Soc. Am.* **1964**, *54* (8), 1031-1040.
- Method of measuring and specifying colour rendering properties of light sources*. CIE Central Bureau: Austria: Commission internationale de l'éclairage, 1995.
- Color Rendering Index For White Light Sources. http://www.architecturalssl.com/sslinteractive/media/256/ArchLED%20CRI_CQS%20mark.pdf (accessed 6-16-2019).

30. Liu, G.-N.; Zhao, R.-Y.; Xu, R.-D.; Zhang, X.; Tang, X.-N.; Dan, Q.-J.; Wei, Y.-W.; Tu, Y.-Y.; Bo, Q.-B.; Li, C., A Novel Tetranuclear Copper(I) Iodide Metal–Organic Cluster [Cu₄(Ligand)₄] with Highly Selective Luminescence Detection of Antibiotic. *Crystal Growth & Design* **2018**, *18* (9), 5441-5448.
31. Lapprand, A.; Dutartre, M.; Khiri, N.; Levert, E.; Fortin, D.; Rousselin, Y.; Soldera, A.; Jugé, S.; Harvey, P. D., Luminescent P-Chirogenic Copper Clusters. *Inorganic Chemistry* **2013**, *52* (14), 7958-7967.
32. Yu, Y.-D.; Meng, L.-B.; Chen, Q.-C.; Chen, G.-H.; Huang, X.-C., Substituent regulated photoluminescent thermochromism in a rare type of octahedral Cu₄I clusters. *New Journal of Chemistry* **2018**, *42* (11), 8426-8437.
33. Hu, G.; Mains, G. J.; Holt, E. M., Correlation of structure and emission in solid state copper(I) complexes; [Cu₄I(CH₃CN)₄(L)₄], L = aniline derivative. *Inorganica Chimica Acta* **1995**, *240* (1), 559-565.
34. Cornelio, J.; Zhou, T.-Y.; Alkaş, A.; Telfer, S. G., Systematic tuning of the luminescence output of multicomponent metal–organic frameworks. *Journal of the American Chemical Society* **2018**, *140* (45), 15470-15476.
35. White, K. A.; Chengelis, D. A.; Gogick, K. A.; Stehman, J.; Rosi, N. L.; Petoud, S., Near-infrared luminescent lanthanide MOF barcodes. *Journal of the American Chemical Society* **2009**, *131* (50), 18069-18071.
36. Cui, Y.; Yue, Y.; Qian, G.; Chen, B., Luminescent Functional Metal–Organic Frameworks. *Chemical Reviews* **2012**, *112* (2), 1126-1162.
37. White, K. A.; Chengelis, D. A.; Zeller, M.; Geib, S. J.; Szakos, J.; Petoud, S.; Rosi, N. L., Near-infrared emitting ytterbium metal–organic frameworks with tunable excitation properties. *Chemical Communications* **2009**, (30), 4506-4508.
38. McLellan, B. C.; Corder, G. D.; Golev, A.; Ali, S. H., Sustainability of the Rare Earths Industry. *Procedia Environmental Sciences* **2014**, *20*, 280-287.



For Table of Contents Only

1
2
3
4
5
6
7
8
9
10
11
12
13
14
15
16
17
18
19
20
21
22
23
24
25
26
27
28
29
30
31
32
33
34
35
36
37
38
39
40
41
42
43
44
45
46
47
48
49
50
51
52
53
54
55
56
57
58
59
60



TOC